Microelectronics Journal 44 (2013) 860–868

Contents lists available at ScienceDirect

Microelectronics Journal

journal homepage: www.elsevier.com/locate/mejo

Finite element analysis of miniature thermoelectric coolers with high cooling performance and short response time

Wei Zhu [a], Yuan Deng [a,*], Yao Wang [a], Anliang Wang [b,*]

[a] Beijing Key Laboratory for Advanced Functional Materials and Thin Film Technology, School of Material Science and Engineering, Beihang University, Beijing 100191, China
[b] School of Astronautics, Beihang University, Beijing 100191, China

ARTICLE INFO

Article history:
Received 8 November 2012
Received in revised form
20 June 2013
Accepted 24 June 2013
Available online 16 July 2013

Keywords:
Thermoelectric cooler
Finite element methods
Size effect
Cooling performance
Response time

ABSTRACT

The miniature thermoelectric cooler (TEC) is a promising device for microelectronics applications with high cooling performance and short response time. In this paper, a comprehensive numerical analysis focusing on the cooling performance and response time of the TEC is performed by finite element methods (FEMs). The effects of load current, geometric size, ratio of length to cross-sectional area and substrate's thermal resistance on the performance of the TEC are studied. The results show that the performance of TECs has been improved by reducing the TEC's size and ratio of length to cross-sectional area, resulting in a maximum cooling temperature difference of 88 °C, a cooling power density of 1000 W cm^{-2} and a short response time on the order of milliseconds. Furthermore, the substrate, which hinders the circulation of heat between the TEC and the atmosphere, also has a significant influence on the performance of the TEC.

1. Introduction

As the feature size of microelectronic devices decreases, very large amounts of heat are generated in very small areas (also called hot spots). Meanwhile, the higher degree of integration of electronics leads to extreme heat flux densities, which prevents the improvement in electronic performance. Therefore, thermal management to ensure that the integrated chips are kept within their operating temperature limits has become crucial [1–4]. Many cooling techniques for microprocessors, such as air cooling and refrigeration, have been proposed in recent years. Among these, the thermoelectric cooler (TEC) is considered to be a potential candidate with high dissipating abilities and a small size. Furthermore, miniaturized thin-film TECs deliver higher cooling power densities than conventional bulk coolers do, and they can serve as excellent coolers for addressing hot spots [5–11].

The performance of TECs is primarily characterized by the following three parameters: the maximum cooling temperature difference, the maximum cooling power or cooling power density and the response time. On the one hand, the performance of the TEC is related to the thermoelectric performance of the materials evaluated by the dimensionless figure of merit (ZT). The value of ZT is a dimensional parameter, which is defined as

$$ZT = \frac{\alpha^2 \sigma}{\kappa} T \quad (1)$$

where α, σ, κ, and T are the Seebeck coefficient, the electrical conductivity, the thermal conductivity and the absolute temperature, respectively. Although there is no theoretical limitation for ZT, thermoelectric bulk materials have not significantly exceeded ZT~1 for nearly 50 years. The research efforts in the field of thermoelectric thin films increased substantially in the last few years to achieve a high ZT value by enlarging the Seebeck coefficient and the electrical conductivity and reducing the thermal conductivity. The increase of ZT leads directly to an improvement in the cooling power density and the cooling temperature difference [12–15], which are two of the three important parameters used to characterize the performance of TECs. The best materials at room temperature for TECs are bismuth telluride-related compounds [13,15]. Bottner [16] has developed a micro-structured thin-film TEC based on bismuth telluride-related compounds that was fabricated on a silicon substrate with micro-electromechanical system (MEMS) technologies, and a maximum cooling power density of 100 mW cm^{-2} was obtained. On the other hand, optimizing the TEC size dimension is an alternative strategy to achieve high cooling performance. Moreover, development of a theoretical model and finite element methods (FEMs) for predictions of the behaviors of the thermoelectric devices is also essential to improve the performance of these devices [17,18]. As for FEM, it is systematic and efficient to handle very complex geometry, restraints and loading, and it can be divided into a set of logical steps

* Corresponding authors. Tel.: +86 10 8231 3482; fax: +86 10 8233 9431.
E-mail addresses: dengyuan@buaa.edu.cn (Y. Deng), wanganliang@buaa.edu.cn (A. Wang).

0026-2692/$ - see front matter © 2013 Elsevier Ltd. All rights reserved.
http://dx.doi.org/10.1016/j.mejo.2013.06.013

Nomenclature

A	area (m^2)
C	specific heat capacity ($J\ kg^{-1}\ K^{-1}$)
d	thickness (m)
D	electric flux density ($C\ m^{-2}$)
E	electric field intensity ($V\ m^{-1}$)
h	depth (m)
I	current (A)
J	electric current density ($A\ m^{-2}$)
Q	cooling power (W)
q	cooling power density (heat flux) ($W\ m^{-2}$)
R	resistance (Ω)
T	temperature (K)
U	electrostatic potential (V)

Greek symbols

ρ	density ($kg\ m^{-3}$)
α	Seebeck coefficient ($V\ K^{-1}$)
λ	thermal conductivity ($W\ K^{-1}\ m^{-1}$)
κ	thermal conductivity ($W\ K^{-1}\ m^{-1}$)
σ	electric conductivity ($S\ m^{-1}$)
ϕ	electric scalar potential (V)
ε	dielectric permittivity ($F\ m^{-1}$)
Δ	temperature difference (K)
γ	length to cross-sectional area ratio (cm^{-1})

Subscript

c	cold side
h	hot side
n	n-type
p	p-type

which can be implemented on a digital computer and utilized to solve three dimensional problems with a very good accuracy and a short solution time. Also, after solution, we could extract relative data of temperature, heat flux and so on from any place in the model. Hence, the numerical simulation methods can yield detailed solutions that are not easily obtained through experiments and provide information to guide the design of TEC devices [18]. In the study of Huang et al. [19], micro-thermoelectric coolers suitable for localized hot-spot cooling applications were successfully fabricated using IC-compatible MEMS technology. Goncalves et al. [20] further reported theoretical modeling, FEM simulations, details of the fabrication process and preliminary results for the first on-chip thermoelectric microcooler array, and a temperature difference of 15 K could be achieved in each pixel. Additionally, a numerical analysis of a micro-cooler has been conducted by Lee et al. [21] and Pérez-Aparicio et al. [22] to determine the effect of the thermoelectric and electrical properties of the material on the cooling performance. Kim et al. [7] and Wu et al. [23] then discussed the effect of the thickness and the width-to-depth ratio on the performance of TECs. Chen et al. [24] also performed a numerical study on the performance of thermoelectric coolers affected by the Thomson effect.

The response time, as illustrated above, is another important parameter used to characterize the performance of TECs. It plays a vital role in the fast cooling of quick-response objects, such as IR detectors, various sensors and miniature semiconductor lasers. The response time of common bulk TECs is generally several seconds. The realization of a short response time can accelerate sensors, stabilize emitters and also open up a variety of new opportunities for TEC applications. Commonly, the response time of TECs is evaluated by a Harman-like measurement [25]. However, the testing device is complicated and requires calibration prior to use. By miniaturizing the TECs, the response time is greatly decreased, which introduces additional precision and accuracy challenges in the test. Therefore, there is a substantial need for a simpler method to investigate and predict the response times of TECs.

For TEC devices, the ratio of length to cross-sectional area is an important dimensional parameter because the internal electrical resistance and thermal resistance are constant when the ratio of length to cross-sectional area of the TEC is fixed. Thus, comparisons between different TEC sizes at fixed ratios of length to cross-sectional area become more practical. In the studies introduced above, this parameter has been ignored; only the geometrical properties of thickness and the width-to-depth ratio have been considered. Furthermore, due to the application of TECs in the fields of fast cooling and sensors, the device parameter of response time requires more consideration at present. However, it needs relatively large amount of calculation and solution time to obtain the steady-state behavior of TEC through the theoretical equations, and it is even more difficult to obtain the transient-state behavior of TEC through the theoretical calculation. Therefore, few investigations have been conducted on the response time of TECs and we hope to use this powerful numerical technique to analyze the steady-state and transient-state performance of TEC to obtain the cooling performance and response time of TEC, respectively. Particular emphasis is placed on the effects of the ratio of the length to cross-sectional area, the load current and the geometric size on the cooling performance and response time to obtain an optimal TEC design. Moreover, substrate thermal resistance is taken into account by considering the real working conditions of the TEC, and subsequently, the effect of the specific electrical contact resistance is also discussed.

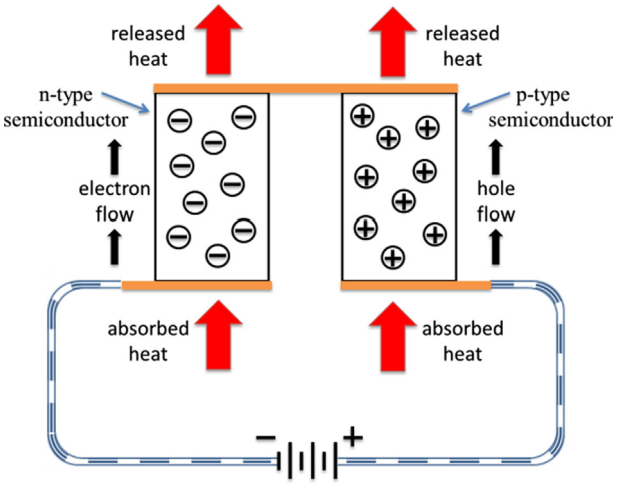

Fig. 1. Working principles of TEC.

2. General description of the TEC performance

The TEC consists of two semiconductor elements connected by a metal strap. When a current flow is applied to one end, as seen in Fig. 1, the motions of the holes in the p-type semiconductor and the electrons in the n-type semiconductor are consistent with the current direction. Meanwhile, the heat is pumped by the carriers from the cold side to the hot side of the thermocouple.

The TEC works in the following two typical ways to achieve different cooling purposes: maximum temperature (also maximum cooling power) and maximum coefficient performance [26]. For the maximum temperature difference approach, the current is determined by

$$I = \frac{|\alpha_n| + |\alpha_p|}{R_t} T_c \tag{2}$$

The cooling power and temperature difference can be obtained from the following equations:

$$Q_c = (|\alpha_n| + |\alpha_p|)T_c I - \frac{1}{2} I^2 (R_e + R_t) - \kappa(T_h - T_c) \tag{3}$$

$$\Delta T = \frac{(|\alpha_n| + |\alpha_p|)T_c I - (1/2) I^2 (R_e + R_t) - Q_c}{\kappa} \tag{4}$$

where α_p and α_n are the Seebeck coefficients of p-type and n-type thermoelectric materials, respectively. I represents the current. T_h and T_c represent the temperatures of the hot side and cold side, respectively. R_t is the electrical resistance of the thermoelectric couple, and R_e is the electrical resistance of the electrodes. Under real circumstances, a contact resistance (R_c) exists between the semiconductor element and the electrode. Therefore, Eq. (3) should be corrected to

$$Q_c = (|\alpha_n| + |\alpha_p|)T_c I - \frac{1}{2} I^2 (R_e + R_t + R_c) - \kappa(T_h - T_c) \tag{5}$$

Actually, the cooling power per unit area is a parameter with more importance for TEC and the cooling power density on the cold side of TEC is obtained by

$$q = Q_c / A_c \tag{6}$$

where A_c represents the cold-side area of the TEC.

3. Mathematical formulation and modeling

3.1. Governing equations

The numerical simulation was performed by using the commercial software ANSYS (Version 12.1), which supports thermal-electric multiphysics analyses. In a thermoelectric analysis, the equations of heat flow and electric charge are expressed as

$$\rho C \frac{\partial T}{\partial t} + \nabla \cdot \vec{q} = \vec{J} \cdot (-\nabla U) \tag{7}$$

$$\nabla \cdot \left(\vec{J} + \frac{\partial \vec{D}}{\partial t} \right) = 0 \tag{8}$$

where ρ, C, $\vec{q}$ and V represent the density, the specific heat capacity, the heat flux vector and the electrostatic potential, respectively. $\vec{J}$ is the electric current density vector, and $\vec{D}$ is the electric flux density vector, which can be derived from $D = \varepsilon E$, where ε is the dielectric permittivity.

The above two equations are coupled by the set of thermoelectric constitutive equations [27]:

$$\vec{q} = \alpha T \vec{J} - \kappa \nabla T \tag{9}$$

$$\vec{J} = \sigma(\vec{E} - \alpha \nabla T) \tag{10}$$

Substituting Eqs. (9) and (10) into Eqs. (7) and (8) produces a system of coupled equations of thermoelectricity:

$$\rho C \frac{\partial T}{\partial t} + \nabla \cdot (\alpha T \vec{J}) - \nabla(\kappa \nabla T) = \vec{J} \cdot (-\nabla U) \tag{11}$$

$$\nabla \cdot \left(\varepsilon \nabla \frac{\partial \varphi}{\partial t} \right) + \nabla \cdot (\sigma \alpha \nabla T) + \nabla \cdot (\sigma \nabla \varphi) = 0 \tag{12}$$

where $\vec{E} = -\nabla \varphi$ is the electric field intensity vector, and φ is the electric scalar potential. In this paper, the elements of Solid 226 and Solid 227 in ANSYS were chosen to conduct the thermal-electric coupling field analysis, which support the Joule heat transfer analysis and thermoelectric effect analysis, such as the Peltier effect and Seebeck effect. At the same time, they both support the steady-state and transient-state analysis. Hence, we use ANSYS Parametric Design Language (APDL) to compile the program code to finish fulfill the numerical simulation of TEC. Particularly for the transient-state analysis, it also called time-history analysis, which is a technique used to determine the dynamic response of a structure under the action of any general time dependent loads. This type of analysis is used to determine the time-varying temperature, displacements, stress and so on. In the solution procedure, transient analysis was applied to obtain the time-varying temperature of TEC, and in the post-processing procedure, the time dependent temperature data of required notes in TEC model were exported to deal with transient-state analysis.

3.2. Geometric model

The TEC module is composed of a ceramic substrate, a copper strip and thermoelectric unicouples, as shown in Fig. 2a. Normally,

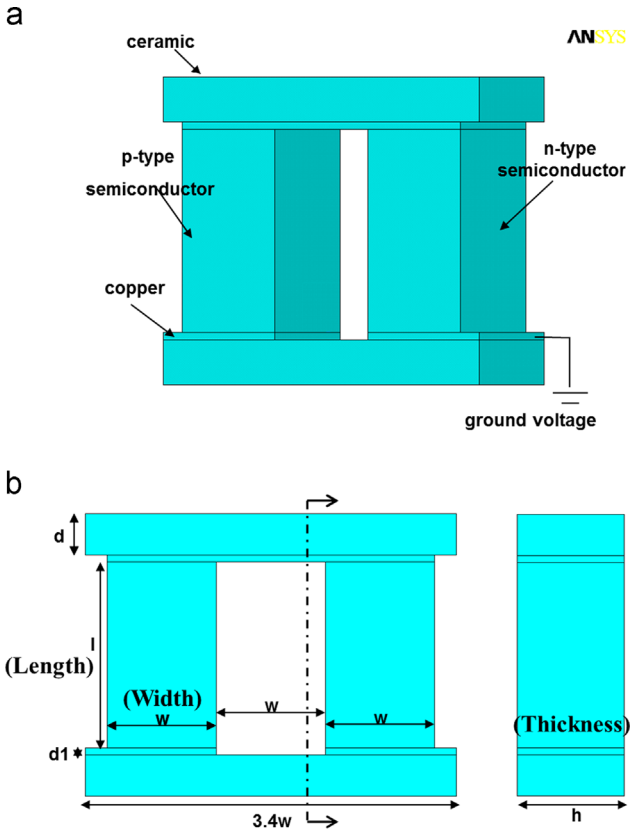

Fig. 2. (a) Scheme of the thermoelectric module; (b) geometric size characterization of the thermoelectric unicouple.

Table 1
Material properties of the thermoelectric module [23,27].

Material properties	Seebeck coefficient ($V K^{-1}$)	Resistivity (Ω m)	Thermal conductivity ($W K^{-1} m^{-1}$)	Density ($kg m^{-3}$)	Heat capacity ($J kg^{-1} K^{-1}$)
n-Type material	−200e−6	1e−5	1.0	7740	154.4
p-Type material	200e−6	1e−5	1.0	7740	154.4
Copper strip	6.5e−6	1.67e−8	400	8920	385

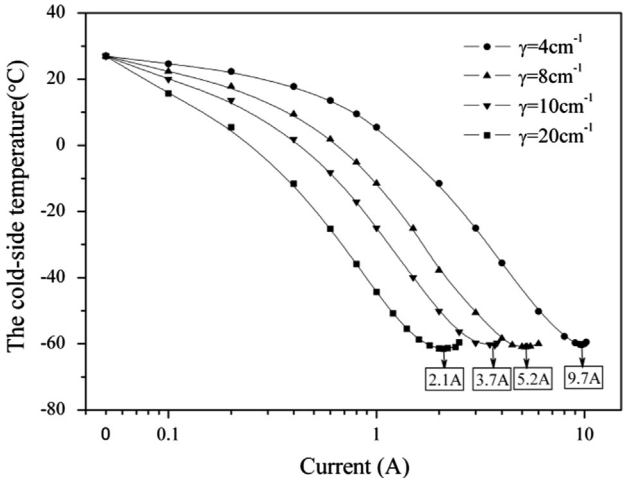

Fig. 3. Current-dependent cold-side temperature of TECs with different ratios of length to cross-sectional area.

a pair of thermoelectric unicouple assemblies is considered as a unit for performance estimation [28]. Fig. 2b indicates the geometric size characterization of the unicouple. The length of TEC depends on the value of w and the cross-sectional area the product of TEC's width and thickness. The material properties, such as the Seebeck coefficient, thermal conductivity, resistivity, density and heat capacity, are all kept constant and are summarized in Table 1.

4. Results and discussion

4.1. Cooling performance of the TEC

4.1.1. Effect of the load current

The hot-side temperature of the TEC was fixed at 27 °C, and different currents were applied to the TEC. Fig. 3 shows that the cold-side temperature depends on the imposed current. With an increase in the current, the cold-side temperatures of the TEC modules all drop rapidly at first because the Peltier heat ($\alpha I T_c$), which is proportional to the current, increases rapidly. Thus, the heat is quickly pumped from the cold side to the hot side of the TEC. However, the continually increasing current will produce much more Joule heat (I^2R), which is proportional to the square of the current. In turn, the heat flux will be conducted to the cold side and suppress the cooling. Therefore, the TEC has an optimal working current to achieve the maximum temperature difference. From Fig. 3, the optimal working currents are obtained at different ratios of length to cross-sectional area. When the ratios are 4 cm^{-1}, 8 cm^{-1}, 10 cm^{-1} and 20 cm^{-1}, the optimal working currents are 9.7 A, 5.2 A, 3.7 A and 2.1 A, respectively. Moreover, the lowest cold-side temperatures are almost equal for TECs with different geometric dimensions at their respective optimal working currents.

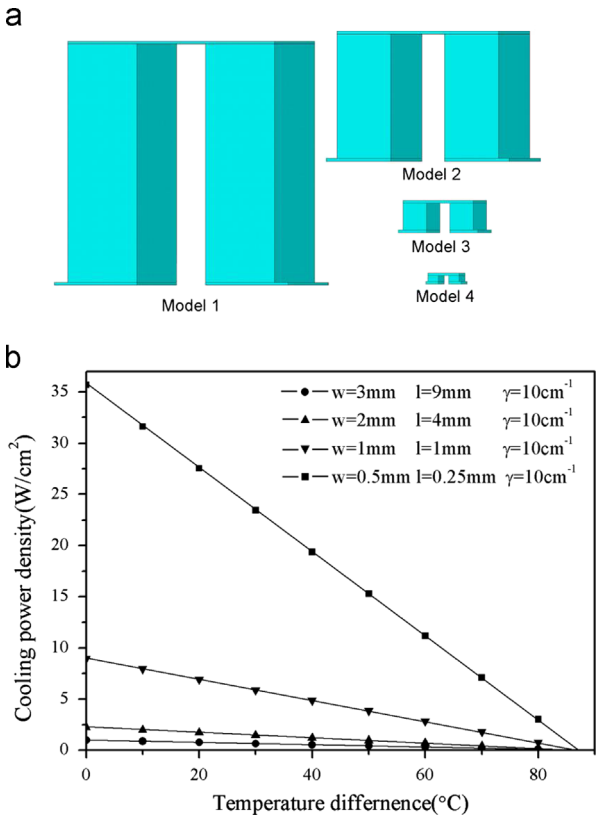

Fig. 4. (a) Scheme of the thermoelectric unicouples with different geometric sizes; (b) load lines of the thermoelectric models with different geometric sizes. The working current is 3.7 A.

Table 2
Geometric size of the thermoelectric unicouple.

	d (mm)	$d1$ (mm)	l (mm)	w (mm)	h (mm)	γ (cm^{-1})
Model 1	0	0.1	9	3	3	10
Model 2	0	0.1	4	2	2	10
Model 3	0	0.1	1	1	1	10
Model 4	0	0.1	0.25	0.5	0.5	10

4.1.2. Effect of the geometric size

To study the effect of the geometric size on the performance of the TEC, four different models were established, as shown in Fig. 4 (a). With the development of precision machine technology, the fabrication of sub-millimeter bulk thermoelectric legs is becoming a reality. Thus, the length to cross-sectional area ratio of the thermoelectric module was fixed at 10 cm^{-1}, and the width was decreased from 3 mm to 0.5 mm. The specific size characteristics are illustrated in Table 2. The substrate was not taken into consideration. The same

boundary conditions were applied to the TEC, and the working current was loaded at its optimal value of 3.7 A.

Generally in the measurement, the temperature difference across the TEC would decrease with the increase of the heat load applied on the cold-side of TEC. When the heat load increases to a specific value, the temperature difference will decrease to zero, and now the power of heat load can be thought as the maximum cooling power of TEC. Similarly, when the heat load is zero, the maximum cooling temperature difference of TEC is obtained. It should be illustrated that the maximum cooling power (or the maximum cooling power density) and the maximum cooling temperature difference are only two parameters used to characterize the performance of TEC. They represent two different working conditions, which could not be obtained simultaneously. Considering the practicality in the numerical simulation, the temperature loaded on the cold-side is varied in this paper, and then heat flux data of cold-side nodes in TEC model were collected, which could be considered as the cooling power density of TEC. By plotting the cooling power density as a function of the temperature difference at a fixed operating current, the load line is generated which is the most common measurement of TEC's performance. The temperature difference at zero q is referred to as ΔT_{max}, and the cooling power density at zero ΔT is referred to as q_{max}. ΔT_{max} and q_{max} define the performance envelope of a TEC and are often used as a basis of comparison. Fig. 4(b) illustrates the load lines of the above four models. From Fig. 4(b), the maximum temperature difference appears to be almost the same (88 °C), while the cooling power density increases significantly with the size reduction. When the width of the TEC module is 0.5 mm, the cooling power density is approximately 36 W cm^{-2}, which is nearly 36 times larger than that of the TEC at $w=3$ mm. For $w=1$ mm and $w=2$ mm, the cooling power densities are approximately 9 W cm^{-2} and 2 W cm^{-2}, respectively. Therefore, the cooling power density differs considerably when the cold-side areas of the TECs are varied.

Based on the simulation results, it can be determined that the cooling power density increases significantly with the size reduction of the TEC. According to Eq. (3), the TECs with the same ratio of length to cross-sectional area have the same cooling power under a certain condition. Thus, TEC with smaller size would deliver a higher cooling power density. In addition, the rapid expansion of microelectronics technology requires thermal management solutions and makes the miniaturization of TECs an urgent issue. With the development of micro-electromechanical system technologies, TECs with a thermoelectric module width of less than 100 μm can now be fabricated. Therefore, the size of TECs continues to decrease, with the width decreasing from 0.4 mm to 0.1 mm, as shown in Table 3. Because the width is 0.1 mm, the cooling power density increases to as much as 1000 W cm^{-2}, which is quite large considering the current performance of TECs.

Table 3
Cooling performance comparison of the cooling power density between models 1–4 and models 5–8.

$\gamma=10$ cm^{-1}, $I=3.7$ A, $Q_c=0.3$ W	w (mm)	l (mm)	h (mm)	q (W cm^{-2})
Model 1	3	9	3	0.99
Model 2	2	4	2	2.24
Model 3	1	1	1	8.97
Model 4	0.5	0.25	0.5	35.68
Model 5	0.4	0.16	0.4	63
Model 6	0.3	0.09	0.3	111
Model 7	0.2	0.04	0.2	250
Model 8	0.1	0.01	0.1	1000

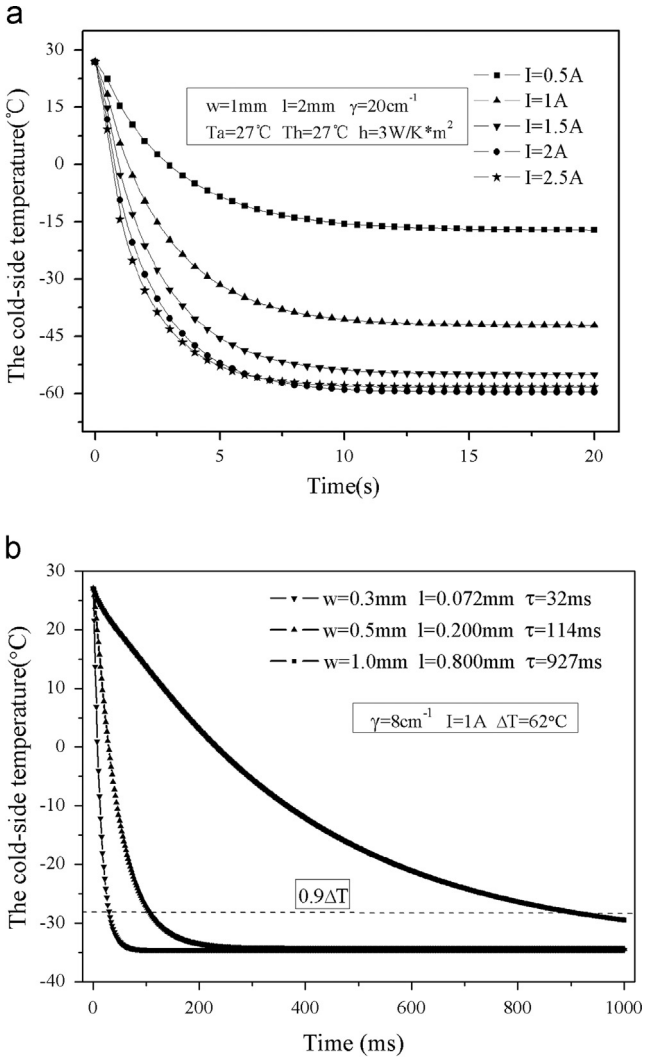

Fig. 5. (a) Time-dependent cold-side temperature of the TEC using different currents. (b) Time-dependent cold-side temperature of TECs with different geometric sizes. The time (τ) required to achieve $\Delta T=0.9\Delta T_{max}$ is defined as the response time of the TEC.

Table 4
Cooling performances of TECs with different ratios of length to cross-sectional area.

	$\gamma=4$ cm^{-1}		$\gamma=8$ cm^{-1}		$\gamma=10$ cm^{-1}		$\gamma=20$ cm^{-1}	
	q (W cm^{-2})	ΔT (°C)	q (W cm^{-2})	ΔT (°C)	q (W cm^{-2})	ΔT (°C)	q (W cm^{-2})	ΔT (°C)
$w=0.5$ mm	89.67	86.68	47.06	87.31	35.68	87.59	14.88	88.36
$w=1$ mm	22.68	87.08	11.85	87.51	8.97	87.78	4.79	88.47
$w=2$ mm	6.72	87.15	3.85	87.60	2.24	87.83	1.20	88.51
$w=3$ mm	2.99	87.17	1.58	87.63	0.99	87.85	0.53	88.52

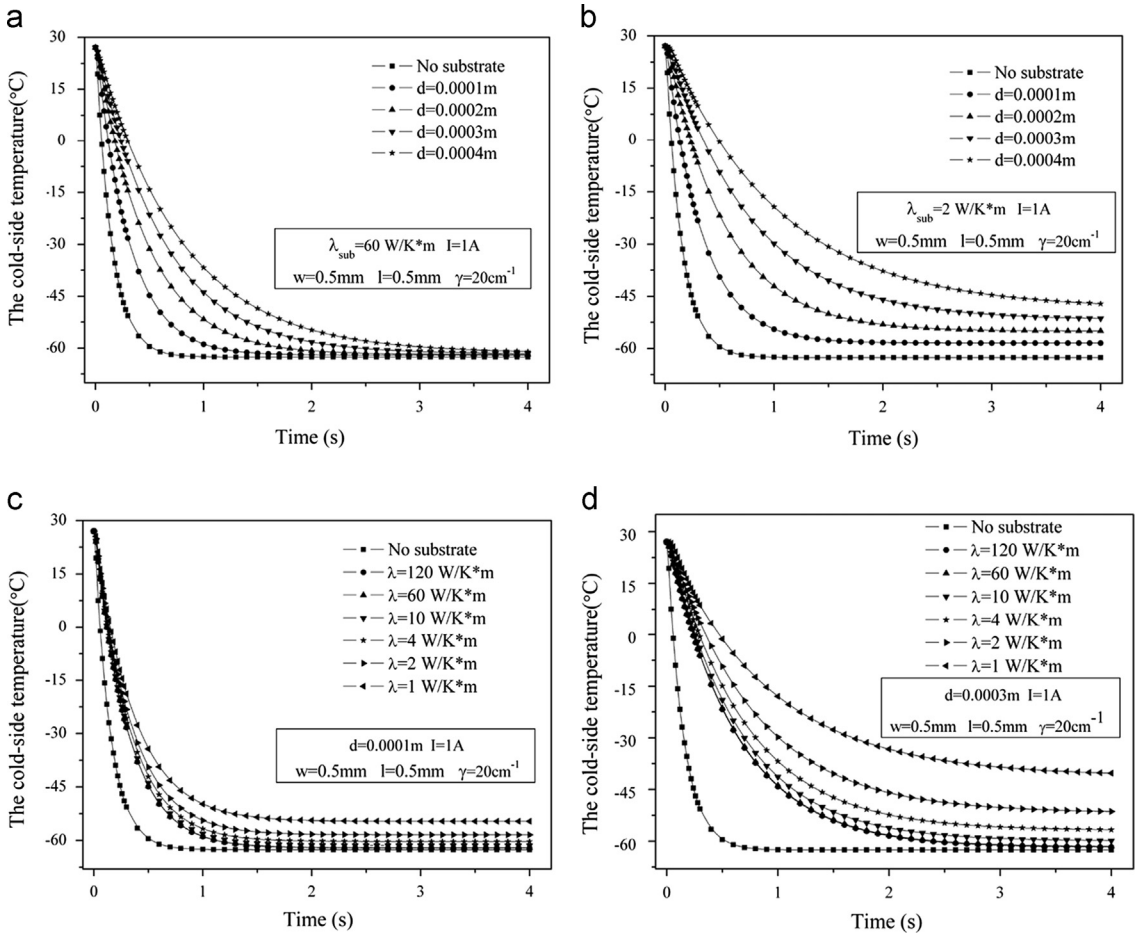

Fig. 6. Time-dependent cold-side temperature of TECs with different substrate thicknesses: (a) the thermal conductivity is 60 W K^{-1} m^{-1}; (b) the thermal conductivity is 2 W K^{-1} m^{-1}. Time-dependent cold-side temperature of TECs with different substrate thermal conductivities: (c) the thickness is 0.1 mm; (d) the thickness is 0.3 mm.

4.1.3. *Effect of the length to cross-sectional area ratio*

The ratio of the length to the cross-sectional area of the TEC is a vital dimensional parameter for establishing a constant internal electrical resistance and thermal resistance with a fixed ratio of length to cross-sectional area in TECs. TEC models with different ratios of length to cross-sectional area were simulated, and the maximum temperature differences and cooling power densities are summarized in Table 4. For ratios of 4 cm^{-1}, 8 cm^{-1}, 10 cm^{-1} and 20 cm^{-1}, the maximum temperature difference across the TEC remains 88 °C, which agrees with the conclusion based on Fig. 3. Similar to the TEC at $\gamma = 10$ cm^{-1}, the cooling power density at three other ratios increases with as the dimensional size decreases. In addition, the cooling power density is 36 W cm^{-2} when the ratio is 10 cm^{-1} and the width is 0.5 mm. When the ratio decreases to 4 cm^{-1}, the cooling power density increases to 90 W cm^{-2}. Therefore, the cooling power density is greatly enhanced as the length to cross-sectional area ratio is decreased.

4.2. *Response time of the TEC*

4.2.1. *Effect of the load current*

In addition to the study of the cooling performance of TECs to obtain the maximum cooling temperature difference and the cooling power density for the optimal design, the transient process was also investigated to elucidate the response time of the TEC. Fig. 5(a) shows the time-dependent cold-side temperature of the TEC. The environmental temperature was fixed at 27 °C, and the convection heat transfer coefficient was kept at 3 W K^{-1} m^{-2} between the TEC and the ambient air. Once the current flow is applied to the TEC, the cold-side temperature decreases initially and then converges to a constant that is much lower than the ambient temperature. It is worth noting that this temperature decrease is quite dependent on the operating current. An increase of the current will lead to a more significant Peltier effect, and the temperature will initially decrease more rapidly. However, as time passes, the Joule heat is gradually transported to the cold side, which results in the slow decrease of the cold-side temperature. Because the time-dependent cold-side temperature is strongly influenced by the currents, the same working current of $I = 1$ A was used in the following TEC modules to facilitate comparisons.

4.2.2. *Effect of the geometric size*

Analogous simulations were performed for other TEC modules of different geometric sizes, as shown in Fig. 5(b). The ratio of length to cross-sectional area was fixed at 8 cm^{-1}, and the width was decreased from 1.0 mm to 0.5 mm and 0.3 mm. With the decrease of the width and length, the cooling process becomes faster. However, the maximum temperature difference changes only slightly for the fixed load current and length to cross-sectional area ratio. It is reasonable to consider the time required to reach a specific value of the relation $\Delta T(t)/\Delta T_{max}$ to be the TEC's response characteristic. To create a unified value for comparison of the TEC response time, the time required to achieve $\Delta T = 0.9\Delta T_{max}$ is defined as the response time of the TEC. In Fig. 5(b), the dashed line represents the temperature at $0.9\Delta T_{max}$. When the width decreases from 1.0 mm to 0.5 mm to 0.3 mm, the response times are 927 ms, 114 ms and 32 ms, respectively. Compared with the response time of bulk TECs,

which is on the order of seconds, it is demonstrated that the small-scale TEC has a shorter response time.

4.2.3. Effect of the length to cross-sectional area ratio

The TEC models with different ratios of length to cross-sectional area for different geometric sizes were simulated, and the response times are summarized in Table 5. When the ratios are 4 cm^{-1}, 8 cm^{-1}, 10 cm^{-1} and 20 cm^{-1}, the response times are considerably different. The response times decrease approximately proportionally to the reduction of the ratio of length to cross-sectional area (also the length of the TEC). Thus, when the length of the TEC is reduced, the response time is shorter. Furthermore, the response times of the TEC at three other ratios are analogous with that of a TEC at $\gamma = 8\ cm^{-1}$, and the response times all decrease as the size is reduced. When the ratio is 4 cm^{-1} and the width is 0.3 mm, the response time drops to a minimum of 16 ms. Therefore, it can be determined that the response time of miniature TECs is about one-tenth that of the bulk TEC, and the cooling power density of miniature TECs is ten times greater than that of the bulk TEC. It is obvious that in the practical applications, decreasing of TEC's size is an efficient approach to speed the cooling process and promote the cooling power density.

Table 5
Response times of TECs with different ratios of length to cross-sectional area.

τ(ms)	$\gamma = 4\ cm^{-1}$	$\gamma = 8\ cm^{-1}$	$\gamma = 10\ cm^{-1}$	$\gamma = 20\ cm^{-1}$
w=0.3 mm	16	32	41	83
w=0.5 mm	51	114	163	355
w=1 mm	328	927	2150	5300

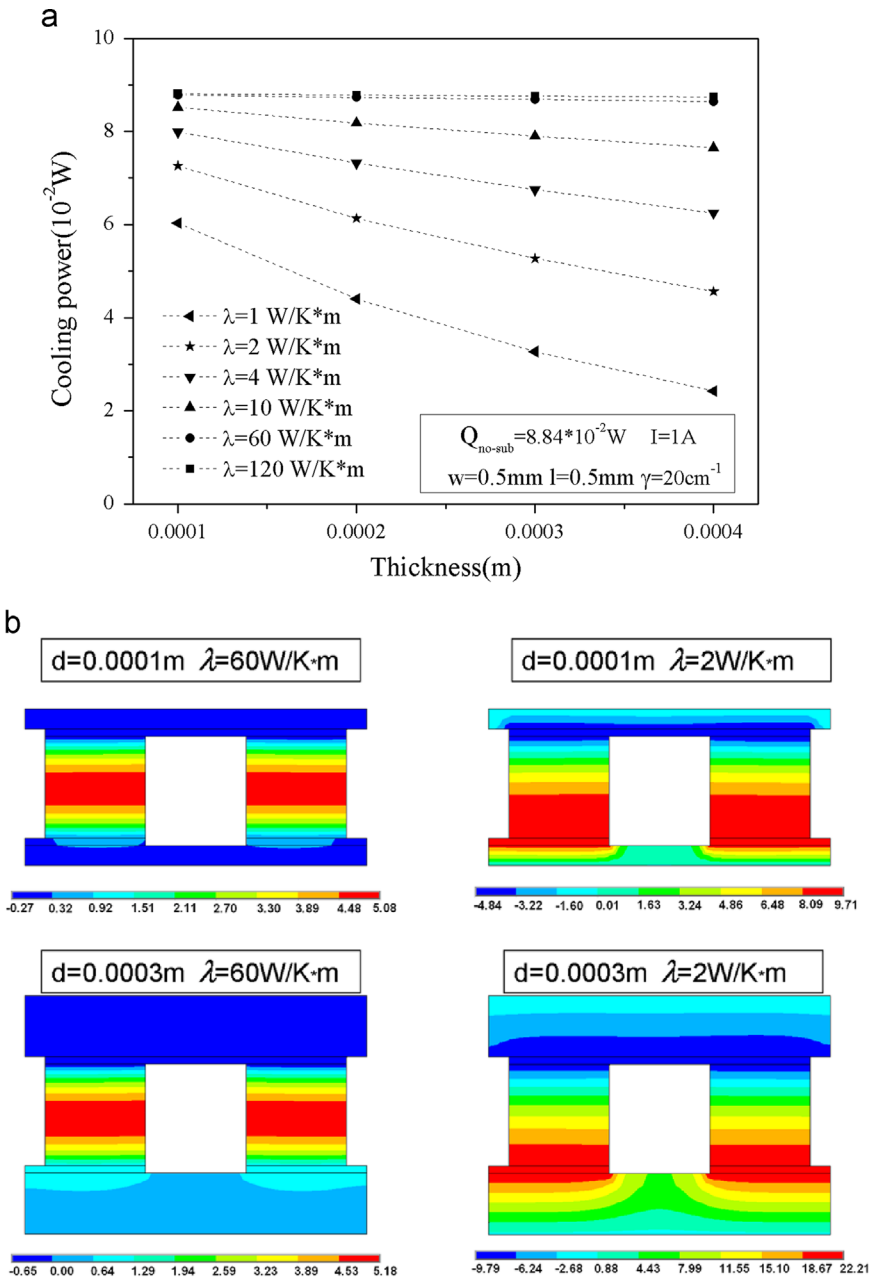

Fig. 7. (a) Cooling power of TECs with substrates with different thermal conductivities and thicknesses. The cooling power is 8.84×10^{-2} W without the substrate. (b) Distributions of temperature (°C) for the thermoelectric FEM model for different thermal conductivities and thicknesses.

5. Performance prediction

5.1. Thermal resistance (substrate)

5.1.1. Effect of thermal resistance on cooling performance

In real conditions, thermal resistance of the substrate and contact resistance between the thermoelectric material and the electrode still exist. When a current is applied to the TEC to pump a heat flow, the heat flow should be released from the hot side of the TEC due to energy conservation. Hence, the characteristics of the substrate must be considered, and substrates with different thermal conductivities and thicknesses were studied in this work. The length and width of TEC are fixed at 0.5 mm and the ratio of length to cross-sectional area is 20 cm^{-1}. A current of 1 A is applied on TEC. The time-dependent cold-side temperatures of the TEC are shown in Fig. 6. As shown in Fig. 6(a), when the thermal conductivity is 60 W K^{-1} m^{-1}, the TECs have essentially the same minimum temperatures for different substrate thicknesses; however, the thickness does impact the cooling to some extent. When the thermal conductivity decreases to 2 W K^{-1} m^{-1}, as shown in Fig. 6(b), the thickness becomes dominant enough to affect the minimum cooling temperature, and when the thickness is 0.4 mm, the maximum temperature difference of the TEC drops by 15 °C compared with that of a TEC without a substrate.

Subsequently, the thicknesses were set at 0.1 mm and 0.3 mm, and the thermal conductivity varied from 1 W K^{-1} m^{-1} to 120 W K^{-1} m^{-1}. The time-dependent cold-side temperatures of the TEC are shown in Fig. 6(c) and (d). Because the heat flow needs to be released from the substrate, the substrate has a considerable impact on the cooling power. However, the cooling power of TECs with substrates with different thermal conductivities does not appear to be substantially different. When the thermal conductivity is greater than 10 W K^{-1} m^{-1}, the minimum temperatures of the TEC remain almost the same for $d=0.1$ mm and $d=0.3$ mm. However, the maximum temperature decreases substantially when the thermal conductivity is less than 10 W K^{-1} m^{-1}.

As shown in Fig. 7(a), besides the effect of the substrate on the cold-side temperature of the TEC, the substrate also affects the cooling power of the TEC. The TEC pumps a cooling power of 8.84×10^{-2} W without the substrate. When the thermal conductivity of the substrate is greater than 10 W K^{-1} m^{-1}, the cooling power is essentially unchanged compared with that of a TEC without a substrate. In contrast, when the thermal conductivity is decreased and the thickness is simultaneously increased, a large decrease of the cooling power of the TEC is observed. From Eq. (3), the maximum cooling power can be obtained because the temperature difference is zero across the TEC. The temperature contours of a TEC with substrate are illustrated in Fig. 7(b). For the condition of $\lambda=60$ W K^{-1} m^{-1}, the temperature distribution is uniform and similar. At this point, the Peltier heat and the Joule heat can be easily released through the substrate, so the maximum temperature occurs in the middle of the TEC. However, for the condition of $\lambda=2$ W K^{-1} m^{-1}, the large thermal resistance hinders the circulation of the heat, leading to the accumulation at the hot side of the heat that has been pumped from the cold side; thus, the maximum temperature occurs on the hot side of the TEC. Even worse, increasing the thickness results in much higher temperature. The temperature increases to 22.21 °C for $d=0.3$ mm compared with 9.71 °C for $d=0.1$ mm.

5.1.2. Effect of thermal resistance on the response time

The substrate is another factor influencing considerably the TEC's quick-responsibility, which is shown in Fig. 8. When the thickness is 0.1 mm and the thermal conductivity is varied, the response times are all less than 1 s, which is comparable to the 0.36 s response time in the ideal condition. Additionally, the response time increases approximately proportionally to the increase in the thickness. Likewise, the response time increases considerably when the thermal conductivity decreases from 120 W K^{-1} m^{-1} to 1 W K^{-1} m^{-1}. When the thickness is 0.4 mm and the thermal conductivity is 1 W K^{-1} m^{-1}, the response time is almost tenfold longer than that of an ideal TEC. It is demonstrated that the substrate is a rather vital factor that exerts considerable influence on the response time of the TEC. Most importantly, to increase TEC performance, a small thickness and a high thermal conductivity of the substrate are necessary for the fabrication of TEC devices.

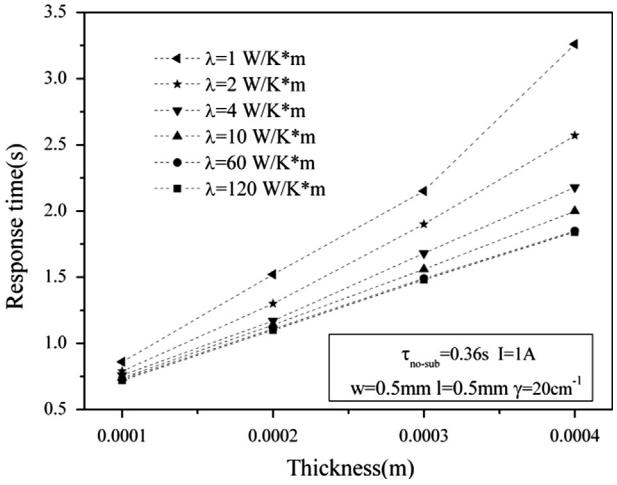

Fig. 8. Response times of TECs with substrates with different thermal conductivities and thicknesses. The response time is 0.36 s without a substrate.

5.2. Contact resistance

In addition to the thermal resistance, the specific electrical contact resistance between the thermoelectric material and the electrode is another important factor affecting the performance of TECs. As a result of the miniaturization of TECs and the high densities of p–n connections in series, the contact resistance can no longer be ignored. The increase of the total resistance, which is contributed to by the electrical contact resistance, has introduced more Joule heat. As a result, the Peltier heat is suppressed, and the heat cooling power decreases according to Eq. (5). Hence, the contact resistance needs to be considered during the fabrication of TEC devices. To provide good working conditions for TECs, the specific electrical contact resistance should typically be maintained under 1e−10 Ω m^{-2} [16,29].

6. Conclusion

In this study, both the cooling performance and the response time of TECs were investigated by FEM to determine the performance of miniature TECs under different working conditions and with different designs. The effects of the TEC working current, size and ratio of length to cross-sectional area, considered as key parameters in the proposed TEC modules, were taken into account. Under the given conditions, there is an optimal working current for TECs with a fixed ratio of length to cross-sectional area. The maximum temperature difference of the TECs is 88 °C at the optimal working current. The analysis results also indicate that the performance of the TEC is greatly improved by decreasing the geometric size and the ratio of the length to cross-sectional area. In the TEC module, when the ratio of the length to cross-sectional

area is less than 10 cm^{-1} and the width is less than 0.5 mm, the cooling power density of the TEC exceeds 100 W cm^{-2}, and similarly, the response time of the TEC falls below 100 ms. Furthermore, the cooling power density of the TEC increases to 1000 W cm^{-2} when the width is reduced to 0.1 mm. This reflects the fact that miniaturizing TECs is an effective route to enhance the cooling performance and shorten the response time of the TECs. Moreover, to avoid heat accumulation and maintain a high TEC performance, substrates with a small thickness and a high thermal conductivity are recommended for use in the fabrication of TECs.

Acknowledgments

This work was supported by the State Key Development Program for Basic Research of China (Grant no. 2012CB933200), the National Natural Science Foundation of China (Nos. 51172008 and 51002006), the National natural science fund innovation group (No. 50921003), the Beijing Technology Topic Program (No. Z111100066511009), the Research Fund for Doctor Station Sponsored by the Ministry of Education of China (20111102110035) and the Fundamental Research Funds for the Central Universities.

References

[1] A.F. Ali, M.S. El-Genk, Spreaders for immersion nucleate boiling cooling of a computer chip with a central hotspot, Energy Convers. Manage. 53 (2012) 259–267.
[2] C. Byon, K. Choo, S.J. Kim, Experimental and analytical study on chip hot spot temperature, Int. J. Heat Mass Transfer 54 (2011) 2066–2072.
[3] J. Kim, Spray cooling heat transfer: the state of the art, Int. J. Heat Fluid Flow 28 (2007) 753–767.
[4] G. Zhang, Q.X. Zhang, D. Kavitha, G.Q. Lo, Time dependent thermoelectric performance of a bundle of silicon nanowires for on-chip applications, Appl. Phys. Lett. 95 (2009) 243104.
[5] I. Chowdhury, R. Prasher, K. Lofgreen, G. Chrysler, S. Narasimhan, R. Mahajan, D. Koester, R. Alley, R. Venkatasubramanian, On-chip cooling by superlattice-based thin-film thermoelectric, Nature Nanotechnol. 4 (2009) 235–238.
[6] B.J. Huang, C.J. Chin, C.L. Duang, A design method of thermoelectric cooler, Int. J. Refrig. 23 (2000) 208–218.
[7] H. Kim, O.J. Kim, K.H. Lee, M. Elimelech, Optimal design of a microthermoelectric cooler for microelectronics, Microelectron. J. 42 (2011) 772–777.
[8] K.H. Lee, O.J. Kim, Analysis on the performance of the thermoelectric microcooler, Int. J. Heat Mass Transfer 50 (2007) 1982–1992.
[9] Y. Pan, B. Lin, J. Chen, Performance analysis of multi-stage thermoelectric coolers, Appl. Energy 84 (2007) 882–892.
[10] H. Zhang, Y. Mui, M. Tarin, Analysis of thermoelectric cooler performance for high power electronic packages, Appl. Therm. Eng. 30 (2010) 561–568.
[11] Y.Y. Zhou, J.L. Yu, Design optimization of thermoelectric cooling systems for applications in electronic devices, Int. J. Refrig. 35 (2012) 1139–1144.
[12] B. Abramzon, Numerical optimization of the thermoelectric cooling devices, ASME J. Electron. Packag. 129 (2007) 339–347.
[13] B. Poudel, Q. Hao, Y. Ma, Y. Lan, A. Minnich, B. Yu, X. Yan, D.Z. Wang, A. Muto, D. Vashaee, X.Y. Chen, J.M. Liu, M.S. Dresselhaus, G. Chen, Z.F. Ren, High-thermoelectric performance of nanostructured bismuth antimony telluride bulk alloys, Science 320 (2008) 634–638.
[14] E. Venkatasubramanian, E. Siivola, T. Colpitts, B. O'Quinn, Thin-film thermoelectric devices with high room-temperature figures of merit, Nature 413 (2001) 597–602.
[15] X.B. Zhao, X.H. Ji, Y.H. Zhang, T.J. Zhu, J.P. Tu, X.B. Zhang, Bismuth telluride nanotubes and effects on the thermoelectric properties of nano-tube-containing nanocomposites, Appl. Phys. Lett. 86 (2005) 062111.
[16] H. Bottner, Micropelt miniaturized thermoelectric devices: small size, high cooling power density, short response time, in: International Conference on Thermoelectrics, Clemson, US, 2005.
[17] B. Jang, S. Han, J.Y. Kim, Optimal design for micro-thermoelectric generators using finite element analysis, Microelectron. Eng. 88 (2011) 775–778.
[18] C.H. Chen, S.Y. Huang, Development of a non-uniform-current model for predicting transient thermal behavior of thermoelectric coolers, Appl. Energy 100 (2012) 326–335.
[19] I.Y. Huang, J.C. Lin, K.D. She, M.C. Li, J.H. Chen, J.S. Kuo, Development of low-cost micro-thermoelectric coolers utilizing MEMS technology, Sens. Actuators A 148 (2008) 176–185.
[20] L.M. Goncalves, J.G. Rocha, C. Couto, P. Alpuim, J.H. Correia, On-chip array of thermoelectric Peltier microcoolers, Sens. Actuators A. 145–146 (2008) 75–80.
[21] K.H. Lee, H. Kim, O.J. Kim, Effect of thermoelectric and electrical properties on the cooling performance of a micro thermoelectric cooler, J. Electron. Mater 39 (2010) 1566–1571.
[22] J.L. Pérez-Aparicio, R. Palma, R.L. Taylor, Finite element analysis and material sensitivity of Peltier thermoelectric cells coolers, Int. J. Heat Mass Transfer 55 (2012) 1363–1374.
[23] K.H. Wu, C.I. Huang, Thickness scaling characterization of thermoelectric module for small-scale electronic cooling, J. Chin. Soc. Mech. Eng. 30 (2009) 475–481.
[24] W.H. Chen, C.Y. Liao, C.I. Hung, A numerical study on the performance of miniature thermoelectric cooler affected by Thomson effect, Appl. Energy 89 (2012) 464–473.
[25] T.C. Harman, J.H. Cahn, J. Logan, Measurement of thermal conductivity by utilization of Peltier-effect, J. Appl. Phys. 30 (1959) 1351–1359.
[26] S.B. Riffat, X. Ma, Optimum selection design of thermoelectric module for large capacity heat pump applications, Int. J. Energy Res. 28 (2004) 1231–1242.
[27] E.E. Antonova, D.C. Looman, Finite elements for thermoelectric device analysis in ANSYS, in: International Conference on Thermoelectrics, Clemson, US, 2005.
[28] G. Chen, Nanoscale Energy Transport and Conversation, Oxford University Press, New York, 2005.
[29] D.M. Rowe, Thermoelectrics Handbook: Macre to Nano, CRC Press, Boca Raton, FL, 2006.